JOURNAL OF CATALYSIS **161,** 766–775 (1996)
ARTICLE NO. 0239

Pentane Conversion on Dealuminated H-Y and HZSM-5

Y. Hong, V. Gruver, and J. J. Fripiat[1]

Department of Chemistry and Laboratory for Surface Studies, University of Wisconsin–Milwaukee, Milwaukee, Wisconsin 53201

Received December 13, 1995; revised March 12, 1996; accepted March 18, 1996

The steady-state rate of *n*-pentane conversion has been related to the Brønsted acidity of dealuminated (D) acid (H) Y zeolites (DHY) and ZSM-5 (DHZ). Low-temperature CO adsorption FTIR detects two kinds of Brønsted sites in DHZ and a distribution of Brønsted sites in DHY. In DHZ no Lewis sites were detected by this technique. In conjunction with results obtained by high-resolution ^{29}Si MAS REDOR spectroscopy and reported elsewhere, a distinction is made between the Brønsted acidity of an OH group bridging a silicon with only one aluminum within its first coordination shell and at least one aluminum in its third shell (Q_1), from an OH group on a silicon with *no* aluminum in its third coordination shell (FAl1). The latter OH group is more acid than the former. In DHY it is shown that the apparent activation energy of the overall *n*-pentane transformation increases to about 110 kJ mol^{-1} as FAl1/Q_1 decreases below 1/3. Above 1/3 the apparent activation energy is about 60 kJ mol^{-1}. The activity of DHY and DHZ scales with FAl1. The selectivity to isomerization vs. cracking depends mainly on the zeolite structure and the partial clogging of the pores by nonframework aluminum.

INTRODUCTION

The activity of a zeolite in hydrocarbon transformation originates from its acidity. The acidity is contributed by an extensive factor, the number of acid sites, and an intensive factor, the acid strength of the individual sites (1). The product of the extensive factor (number of active sites) by the intensive factor (the efficiency of the active sites) should scale the activity (2).

The Brønsted acid center is associated with an OH bridging group in the neighborhood of a tetrahedrally coordinated, framework-aluminum species (1). Because the framework-aluminum atoms are so far apart in high-silica zeolites, it may be expected that all the acid protons would have equal acid strength (3). Thus, the number of the Brønsted acid centers would simply be the number of framework aluminum in the framework. This has been supported by studies involving sorption of bases such as alcohols and amines on H-ZSM-5, H-ZSM-12, and H-mordenites (4), as well as hexane cracking on ZSM-5 (5) or on dealuminated Y (6), where linear increase in activity with framework-aluminum concentration was observed. This suggests that each framework aluminum corresponded to one acid site and all the sites have the same acid strength. However, in low-silica zeolites such as faujasites, the situation is more complicated.

First, a hypothesis has been proposed that the acid strength is under the influence of the whole lattice. The advantage of this approach is that only one kind of site, which averages the strength of all sites, is considered. The number of acid sites is the number of framework aluminum, therefore, the relationship with activity can easily be found. However, microcalorimetric studies showed a distribution of heats of ammonia adsorption from 150 kJ mol^{-1} to less than 100 kJ mol^{-1} with increasing coverage in H-Y zeolites (7), which suggests that the hypothesis of equal strength is not valid. Domains of coverage where the heat of adsorption is quasi-constant have also been observed (8). The severity of the dealumination treatment is undoubtedly at the origin of these apparent contradictions, notwithstanding the influence of the Lewis sites (9).

In a second approach, it is hypothesized that the Brønsted acid sites may have different strengths. For instance, in zeolite Y, sites with different acidity have normally been attributable to the difference in composition or the second coordintion shell of Al in a Si–OH–Al link. The strength increases as the number of next-nearest-aluminum neighbors decreases (10, 11).

The number of aluminum atoms which do not have next-nearest-neighbor aluminum (FAl1) can be obtained from a Monte-Carlo simulation in which the constraint for Al to have no next Al neighbor (Löewenstein rule) has been introduced. FAl is the total number of framework aluminum. For Si/FAl < 4, the Dempsey rule which states that the number of Al–O–Si–O–Al clusters must be minimized should be taken into account. However, the catalysts that we studied had Si/FAl > 3 and only the Löewenstein restriction should apply. In addition, when the Al ordering is perturbed because of the formation of a significant fraction of nonframework aluminum (NFAl), there is no way to calculate the Al distribution by taking the structure into consideration. It has been shown (12) that the numerical results of a Monte-Carlo simulation can be reproduced by calculating

[1] To whom correspondence should be addressed.

0021-9517/96 $18.00

the probability of zero occupancy of next-nearest-neighbor number of sites.

$$\mathrm{FAl1}/(\mathrm{FAl}+\mathrm{Si}) = \alpha(1-\alpha)^{\beta}$$

where $\alpha = \mathrm{FAl}/(\mathrm{FAl}+\mathrm{Si})$ and β is the total number of next-nearest sites. For instance, β is 12 in ZSM-5 and 9 in HY. The number of aluminum atoms, which have one or more Al in the next-nearest coordination shell (FAl_n), is (FAl-FAl1).

Thus, two classes of potentially acidic and distinguishable OH groups linked to FAl1 and FAl_n could be the origin of the Brønsted sites, FAl1 representing much stronger Brønsted acidity than FAl_n.

Assuming that all silicons are framework silicons, the relative amount (per silicon atom) of Si with one Al neighbor was obtained by deconvoluting the ^{29}Si MAS NMR spectrum:

$$Q_1 = \frac{1}{4} \times {}^4Q(1\mathrm{Al}) \Big/ \sum_{n=0}^{n=4} ({}^4Q(n\mathrm{Al})).$$

Q_1 represents the number of OH bridging aluminum to silicon with one aluminum in its first coordination shell. An empirical equation is used to obtain Q_1 from the Si/ASl ratio, namely, $Q_1/\mathrm{Si} = 0.9164/(4.243 + 0.8559 \times \mathrm{Si/FAl})$.

The number of Brønsted sites would be Q_1, while the OH groups linking Si to more than one Al in the Si first coordination shell are less acidic or nonacidic. A recent ^{29}Si CP MAS NMR REDOR study (13), where ^{29}Si is indirectly excited by the protons of chemisorbed NH_3, concluded that NH_4^+ is formed mainly at the expense of bridging OH groups in the link Si–1Al, while OH groups on other links (Si–nAl) with $n > 1$ would hydrogen bond NH_3.

When zeolite is dealuminated by steaming or dry-air calcination, a fraction of the lattice aluminum species is translocated from framework to nonframework positions and upon calcination Lewis acid sites may be formed on these nonframework aluminum species (NFAl). There are numerous examples in the literature which report that the acid activity of zeolites when mildly steamed or dry-air calcined was enhanced as in HZSM-5 (14–16) and in H-Y (17, 18).

A Lewis acid center in zeolite is an electron-deficient site associated with perturbed tetrahedral-coordinated or pentacoordinated aluminum on the NFAl species (19, 20). The number and strength of Lewis acid sites have been studied by FTIR of molecular probes such as pyridine (21) or CO (22, 23). The role of Lewis acidity of NFAl species in hydrocarbon transformations, however, is controversial.

Zholobenko *et al.* (16) believed that the formation of Lewis acid centers on the NFAl species enhances the activity of *n*-hexane cracking. Steamed ZSM-5 with Si/FAl $\simeq$ 35 exhibits an activity enhanced by a large factor, with respect to unsteamed samples in the composition domain 1< FAl/uc/<2.5. Lago *et al.* (15) suggested that pairing an aluminum in the first coordination shell of silicon with one aluminum outside the tetrahedral framework would produce such an enhancement. Ashton *et al.* (14) believed that the synergistic interaction between the Lewis acid sites on NFAl and the Brønsted sites in the framework made the catalyst more efficient, as also suggested for dealuminated mordenites (24).

Indeed, on a set of seven dealuminated H-mordenites in which the numbers of framework Al and of Lewis sites were known, through ^{29}Si MAS NMR and CO FTIR, respectively, it was observed that the initial rate of pentane or *o*-xylene isomerization was proportional to the product of the two Brønsted and Lewis site concentrations (24).

In the dealuminated H-Y (DHY) and HZSM-5 (DHZ) studied in this contribution, it has not been possible to measure the concentration of the Lewis acid centers. In DHY the CO stretching at 2220 cm^{-1} corresponding to the strong Lewis sites (23) was very weak and barely measurable, while in DHZ no CO stretching band corresponding to interaction with Lewis sites was observed. Of course, these negative results do not mean that there are no Lewis sistes in DHZ, but that CO FTIR failed to detect them, either because of their small concentration or because the activation temperature ($\sim$475°C) was not high enough to create them (23).

In spite of the lack of information on Lewis acidity, the study of pentane transformation on DHZ and DHY is, nevertheless, interesting because of important differences in their Brønsted acidity, as explained later on and reported elsewhere (23). Three reactions are going on simultaneously in pentane transformation, namely cracking, isomerization, and disproportionation. The steady-state rate of the total reaction was taken as a measurement of the reactivity.

EXPERIMENTAL

Materials

DHZ samples. Dealuminated HZSM-5 (DHZ) samples were prepared by calcining a parent HZSM-5 sample, from PQ Co. (CBV3020, $SiO_2/Al_2O_3 = 30$, Na_2O wt% = 0.05). The samples labeled DHZ400, DHZ500, DHZ700, DHZ800, and DHZ900 were dealuminated by dry-air calcination for 2 h at 400, 500, 600, 700, 800, and 900°C, respectively. The suffix 400 in DHZ400 refers to the calcination temperature (25).

SDHZ samples. HZSM-5 samples dealuminated by steaming (SDHZ) were prepared by steaming the parent HZSM-5 at 600°C. The HZSM-5 particles were first placed in a vertical quartz tube on a quartz sintered disk. A flow of 40 ml/min He was passing through the disk and the temperature was first increased slowly to 180°C and kept there for 21 h in order to dry the zeolite. The temperature was increased to 600°C at 8°C/min. After 2 h at 600°C, 100 Torr of

water vapor was introduced into the flow, passing through the sample. SDHZ0, SDHZ30, SDHZ150, SDHZ530, and SDHZ1500 are the steamed samples, the steaming time being 0, 30, 150, 530, and 1500 min.

DHY samples. Dealuminated hydrogen-Y (DHY) zeolites were obtained by first exchanging a commercial sodium Y zeolite (PQ Co. CBV100: $SiO_2/Al_2O_3 = 5.1$, Na_2O wt% = 13) nine times with ammonium acetate. The partially exchanged samples were calcined at 400°C for 2 h after the third and sixth exchange in order to increase the degree of ammonium exchange. The samples named DHY400, DHY500, DHY600, DHY700, and DHY800 were prepared by calcining the dried 98% exchanged NH_4Y at 400, 500, 600, 700, and 800°C, respectively. The details of this work was described previously (25).

USYR, DHY600R, DHZ700R, DHM500, and USY. An acid treatment, as described by Wang *et al.* (26), was used to eliminate NFAl formed during the thermal or hydrothermal processes, without affecting the framework aluminum in the zeolite. The conditions were as follows: the zeolite sample was stirred in distilled water with the solid/liquid ratio of 1 g/15 ml at room temperature. In order to avoid supplementary dealumination of the framework, the dropwise addition of diluted hydrochloric acid (0.05 *M*) was stopped when the pH value became about 3.0. The slow pH increase in the stirred solution was corrected by adding HCl again and readjusted to 3.0. The total amount of HCl used depended upon the number of the NFAl species in the sample.

A commercial ultrastable Y (USY, PQ Co., CBV500: $SiO_2/Al_2O_3 = 5.1$, Na_2O wt% = 0.2), as well as DHY600 and DHZ700, were treated by this method. The corresponding samples are called USYR, DHY600R, and DHZ700R. USY and a previously studied dealuminated H-mordenite (DHM500) were used as reference.

Catalysts Characterization

^{29}Si MAS NMR and chemical elemental analysis. The compositions of the catalysts were analyzed by ^{29}Si MAS NMR and chemical elemental analysis, where the Si to framework aluminum (Si/FAl) and the ratio Si to total aluminum (Si/Al) were obtained. From those two ratios and the unit cell chemical composition, the absolute numbers of the framework aluminum and total aluminum were easily obtained.

XRD. In order to estimate the extent of the damage caused by dealumination, the XRD spectra of the hydrated samples were recorded with a Scintag X-ray diffractometer (θ-θ) between 2 and 40°, Cu$K\alpha$ radiation, and 5° per min scanning at room temperature. An NBS standard silicon was used to calibrate the diffraction angle, and in all cases, the 2θ values of the silicon (111) were within less than 0.01° from the theoretical value (28.443°). In the DHY samples, the positions of 111, 220, 311, 331, 511, 440, 533, and 642 reflections were used to calculate the unit cell parameters and the area of 533 was used to estimate the crystallinity of the commercial sodium Y zeolite, CBV100 (25). For ZSM-5, the 011, 200, 012, 031, 051, 033, and 053 reflections were used.

Adsorption isotherms. The full sorption (adsorption and desorption) isotherms of N_2 at 78 K, and pentane at 295 K, on these samples was measured on an automated instrument (Omnisorp 100, Coulter Corporation). Beforehand, the samples were degassed under vacuum (better than 1×10^{-4} Torr) for 2 h at 573 K. The static mode was used in all measurements which were completed within approximately 10 h. The availability of the active sites is estimated from the ratio of the micropore volumes available to pentane and nitrogen.

Surface acidity by CO adsorption FTIR. The detection and estimated concentrations of Brønsted acid sites were carried out using FTIR spectroscopy of CO chemisorption at low temperature (22, 23).

NH_3 chemisorption. Based on ASTM D 4842-88, "Standard Test Method for Determination of Catalyst Acidity by Ammonia Chemisorption" (27), a volumetric NH_3 adsorption system was built in order to measure the total acidity.

The zeolite sample was degassed by heating in vacuum at 400°C and then it was exposed to gaseous ammonia at 175°C (300 Torr in a manifold of 500 cm^3). Keeping the catalyst at the same temperature, the excess ammonia was removed by a trap cooled at liquid nitrogen temperature. Chemisorbed ammonia, either ammonium or ammonia, was calculated from the difference between the standard volume of ammonia before exposure and the volume recovered from the liquid nitrogen trap.

Catalytic Activity

The transformations of pentane and isopentane were carried out in the temperature range of 250 and 350°C in a recirculation system with a total volume of 1.35 liters. Fifty Torr of pentane or isopentane (EM Science, 98%+) in the whole system was mixed with H_2 or He to bring the total pressure to ~1 atm. Pentane or isopentane was dried by activated 4A zeolite and further purified by several freezing–thawing cycles. The measurable impurity was about 0.5% isopentane in pentane and 0.4% pentane in isopentane. The reaction products were analyzed by an on-line gas chromatograph (Perkin–Elmer 8500) with an Alltech Co. column (C-5000 986714L SN#9308A 20 ft × 1/8 in. s.s. p/w V-7 60/80 mesh). The catalytic activity was obtained from the evolution of the degree of transformation vs time. The sampling was made every 30 min. Two examples of the characteristic data are shown in Fig. 1. A linear range can be observed below 15% of transformation and the slope of this linear range is taken as "steady-state rate."

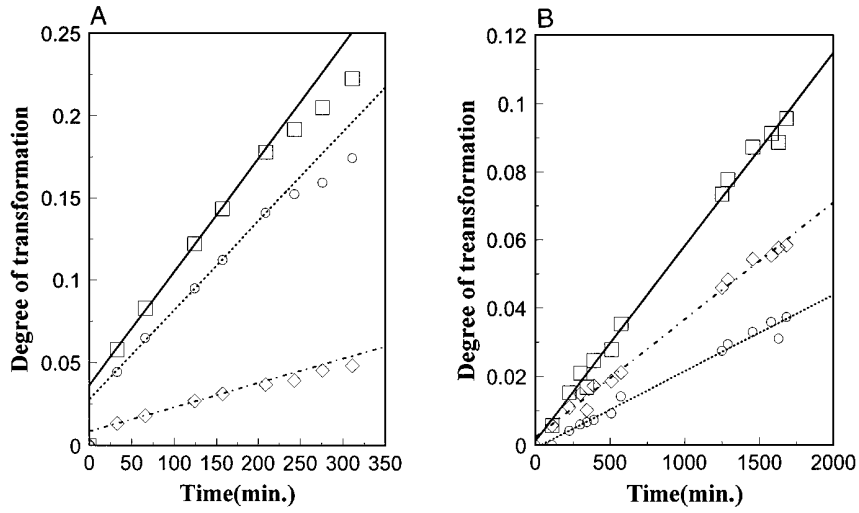

FIG. 1. Examples of the *n*-pentane reaction: degree of transformation vs time. ◯, isomerization; ◇, cracking; and □, total. (A) Temp. 285°C on DHZ400. (B) Temp. 350°C on DHY600.

RESULTS AND DISCUSSION

The numbers of framework aluminum, nonframework aluminum, Si with one FAl in the first coordination shell, and FAl with no Al in the second aluminum coordination shell are listed in Table 1. NFAl is the difference between the number of total aluminum atoms calculated from Si/Al ratio obtained by chemical analysis and the number of FAl obtained by ^{29}Si MAS NMR expressed in atom per gram. It is assumed that all Si atoms belong to the framework. It has been shown earlier that the majority of NFAl are within the zeolite crystal and not outside (25), when dealumination is carried on by calcination.

TABLE 1

Chemical and Structural Compositions Obtained by Chemical Analysis and ^{29}Si MAS NMR

Sample	Si/Al_{CA}	Si/FAl	FAl (10^{20}/g)	NFAl (10^{20}/g)	Q_1 (10^{20}/g)	FAl1 (10^{20}/g)	Avail.
DHZ400	15.1	17.5	5.4	0.81	4.5	2.7	0.904
DHZ500	15.1	17.8	5.3	0.90	4.4	2.7	0.903
DHZ600	15.1	18.6	5.1	1.1	4.3	2.7	0.914
DHZ700	15.1	37.1	2.6	3.6	2.4	1.9	0.892
DHZ800	15.1	52.7	1.9	4.4	1.7	1.5	0.835
DHZ900	15.1	76.3	1.3	4.9	1.2	1.1	0.730
DHM500	5.2	9.8	9.3	6.9	6.0	2.8	0.165
USY	2.55	4.8	17	11	8.0	3.1	0.733
DHY500	2.55	3.29	23	4.9	9.4	2.1	0.735
DHY600	2.55	4.56	18	10	8.2	3.0	0.622
DHY700	2.55	4.81	17	11	8.0	3.1	0.605
DHY800	2.55	4.93	17	11	7.9	3.2	0.410
SDHZ0	15.1	18.6	5.1	1.1	4.3	2.7	0.905
SDHZ30	15.1	19.9	4.8	1.4	4.1	2.6	0.905
SDHZ150	15.1	23.0	4.2	2.0	3.7	2.5	0.905
SDHZ530	15.1	23.6	4.1	2.1	3.6	2.4	0.905
SDHZ1500	15.1	25.3	3.8	2.5	3.4	2.4	0.886
USYR	2.84	4.8	17.1	9.0	9.1	3.1	0.711
DHY600R	3.06	4.56	18.0	6.6	9.2	3.0	0.653
DHZ700R	16.4	37.1	2.6	3.1	2.5	1.9	0.879

Note. FAl and NFAl are the number of framework aluminum and nonframework aluminum, respectively, per gram. Q_1 is the number of silicon with one Al neighbor measured by ^{29}Si MSA NMR, and FAl1 is the number of framework aluminum atoms per gram, which do not have a next-nearest-aluminum neighbor (0.*n.n.n.*Al). Avail. is the fraction of micropore volume measured by pentane with respect to the theoretical lattice mircropore volume.

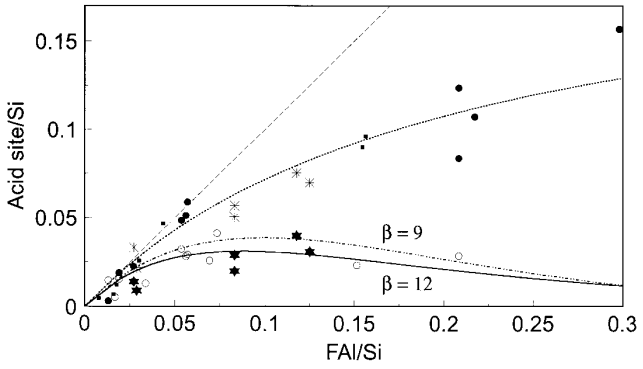

FIG. 2. Comparison between FAl1 ($\beta = 9$ or $\beta = 12$) and the number of acid sites measured by CO low temperature FTIR (◯), Q_1 (···), NH_3 adsorption ASTM test (●), isopropyl-amine TPD-TGA data (■) obtained by Biaglow *et al.* (28), number of NH_3 adsorbed with a residual pressure of 1 Torr (∗), and number of NH_3 adsorbed with heat of adsorption higher than 100 kJ/mol (⋆) obtained by Macedo *et al.* (7). All data are referred to the number of silicon atoms. FAl/Si (- - -) is also shown as reference.

TABLE 2

Number of Chemisorbed Ammonia on DHZ and DHY, According to the ASTM Procedure D4824-88

	NH_3 (10^{20}/g)	
Sample	115°C	175°C
DHZ400	9.99	5.51
DHZ500	8.24	4.80
DHZ600	7.20	4.51
DHZ700	3.16	2.09
DHZ800	2.99	1.69
DHZ900	0.51	0.23
DHY500	18.0	10.6
DHY600	10.4	6.96
DHY700	9.0	5.41
DHY800	5.3	2.80
USY	16.0	9.00

Note. 115 and 175°C are the (ad- and de-)sorption temperatures.

The evolution of FAl1/Si and Q_1/Si (relative value of FAl1 and Q_1) is plotted against FAl/Si in Fig. 2. At low framework aluminum content, Q_1 is practically equal to FAl1; all the bridging OH groups are strong Brønsted sites. This is the composition domain of dealuminated ZSM-5. At the other end, at relatively high content in framework aluminum, such as in dealuminated HY, the total proportion of Brønsted sites (Q_1) is in the order of 1/3 of the amount of FAl and FAl1 is less than 1/3 Q_1. The dealuminated mordenite is in the region when the FAl1 content passes through a maximum, and their proportion is about 50% of Q_1.

In Fig. 2, the region between Q_1 (dotted line) and FAl1 respresents the OH groups bridging Si with one FAl in its first coordination shell and more than one Al in the second Al coordination shell. The region corresponds to Brønsted sites with intermediate strength. The region between FAl (broken line) and Q_1 represents the OH groups linking Si which have two or more FAl in the first coordination shell. They are probably nonacidic, since the NMR REDOR study has shown (13) that these OH do not protonate NH_3.

The amount of acid sites measured by NH_3 chemisorption at 175°C in DHZ and DHY are listed in Table 2. The relative values (with respect to Si) are represented in Fig. 2 by black dots, while results obtained by Macedo *et al.* (7) with NH_3 (Fig. 2, ∗) and by Biaglow *et al.* (28) with isopropylamine (Fig. 2, ■) are shown for the sake of comparison.

Data obtained by Auroux for the amounts of ammonia chemisorbed with heats of adsorption larger than 100 kJ/mol in dealuminated HY are represented in Fig. 2 by (⋆), while (∗) is the amount of NH_3 remaining under 1 Torr NH_3 residual pressure.

The amount of isopropylamine (28) desorbed between 177 and 427°C under vacuum (■) by dealuminated Y, the results of the ASTM test (●), and the values of NH_3 (7) adsorbed with 1 Torr residual pressure (∗) follow Q_1 closely. The NH_3 is a strong base and the amount of adsorbed ammonia should be equal to the toal number of Brønsted acid sites, that is Q_1.

CO is a weak base which can reveal, in favorable cases, different kinds of Brønsted sites as well as Lewis sites (22). For instance, DHZ and USY have two OH populations (23), one corresponding to strong Brønsted sites interacting with CO with the corresponding CO stretch at ~ 2175 cm^{-1}, while the other population yields a broad CO band near 2165 cm^{-1}. The actual values of FAl1 calculated from the experimental integrated absorbance at 2175 cm^{-1} as well as the variation of the number of NH_3 chemisorbed with heats of adsorption larger than 100 kJ/mol are close to the variation of FAl1, with respect to FAl/Si. This strongly supports the hypothesis that the strongest Brønsted sites are OH groups bridging silicon to a 0.*n.n.n.* Al.

The hydrogen-bonded NH_3 is not accounted for in the ASTM test, probably because it cannot stand the treatment at 175°C, as suggestd by the data in Fig. 2. However, the ammonia chemisorbed on Lewis sites should resist this treatment. In DHZ400, 500, 600, and 800, and DHY500, 700, and USY, the difference (NH_3 (175)$-Q_1$) is always positive, and it may account for ammonia on Lewis sites.

Before exposing the catalytic results it should be emphasized that the steady-state rates depicted earlier are not intrinsic rates. Deactivation and coke formation is minor in DHZ samples in the reactions carried out at 285°C in H_2. It is more pronounced under similar conditions on DHY. Carbon analyses of the catalysts have consistently shown that trend. The activity for pentane transformation on calcined DHZ samples at 285°C in H_2 or He, the selectivity toward isomerization, and the ratio of the activity in H_2 over that in He are listed in Table 3.

TABLE 3

Activity of DHZ (ACT-H_2, ACT-He) or Steady-State Rate of Pentane Transformation

Sample	ACT-H_2 Total	ACT-H_2 Iso	ACT-H_2 Crack	Sel-Iso (%)	ACT-He Total	ACT-He Iso	ACT-He Crack	Sel-Iso (%)	H_2/He
DHZ400	25	2.7	21	10.7	19	1.5	18	8.0	1.31
DHZ500	22	2.4	19	10.8	26	2.9	22	11.1	0.85
DHZ600	15	1.7	11	11.6	18	1.7	13	9.4	0.83
DHZ700	12	1.5	10	12.3	9.1	0.89	7.7	9.7	1.32
DHZ800	1.6	0.2	1.3	12.6	1.6	0.16	1.4	10.0	1.0
DHZ900	0.11	0.015	0.080	12.9	0.18	0.007	0.17	4.0	0.61
DHM500	3.7	1.5	1.8	39.6	–	–	–	–	–
USY	2.6	1.7	0.67	63.9	3.0	1.7	1.0	67.9	0.87

Note. Iso, crack, and total are the activity for isomerization, cracking, and total activity at 285°C (unit 1×10^{18} molecule per minute per gram), respectively. Sel-Iso is the selectivity to isomerization. H_2/He is the ratio of the total activity in H_2 over that in He. DHM500 and USY are used for comparison.

The activity decreases with the increasing calcination temperature in DHZ. Since the number of Lewis acid sites is barely measurable in DHZ and in DHY, with CO adsorption we have to credit the activity to the Brønsted acid sites in first approximation. The activity is plotted against Q_1 and the number of FAl1 in Fig. 3 for DHZ. The dispersion of the experimental results is slightly better in Fig. 3A than in Fig. 3B and the substitution of H_2 by He has no noticeable effect.

In all cases, the availability (ratio of condensed volume of pentane over the theoretical micropore volume, see Table 1) must be considered; therefore, either FAl1 or Q_1 is multiplied by the availability (24).

The data for DHY are summarized in Table 4, where the steady-state rates at 285 and 350°C, the selectivity to isomerization, and the activation energy for total transformation are listed. The data for steamed samples and the samples after partial removel of NFAl are listed in Table 5.

The linear relationships (Fig. 3) between the steady-state rates and both the total number of Brønsted sites (Q_1) or the number of strong Brønsted sites (FAl1) observed in DHZ

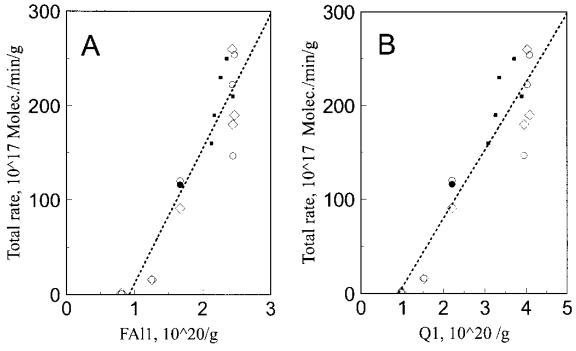

FIG. 3. Plot of total steady-state rate of *n*-pentane conversion vs FAl1 (A) and Q_1 (B) on DHZ calcined in H_2 (◯), or in He (◇), steamed (■), and NFAl partially removed (●).

is easily understood. In the region of high Si/Al ratio, FAl1 varies almost linearly with Q_1 (Fig. 2). The result is that no conclusion can be reached concerning the strength of the acid sites ruling the *n*-pentane transformation on DHZ. In order to obtain information on that matter, data on catalysts with FAl/Si ratios located on both sides of the maximum of FAl1 in Fig. 2 should be available.

The best candidates to yield these data are DHY zeolites. Unfortunately, as shown in Table 1, our samples are near the maximum and the distribution of composition is narrow. The experimental data obtained by Sohn *et al.* (6) for the cracking of *n*-hexane on "D-Y" samples at 350°C can be compared to those shown in Table 4. The large compositional domain was obtained by $SiCl_4$ dealumination with the result that there was less NFAl in Sohn's samples than in ours. Sohn *et al.*'s (6) data were obtained with a continuous-flow reactor in contrast with the recirculation reactor used by us.

Figure 4 shows the variation of the activity vs the number of FAl/uc, Q_1/uc, or FAl1/uc. Our data are corrected by the factor scaling the availability of the site. The activity for the cracking of hexane goes through a maximum if represented vs FAl/uc. In fact, there is a sharp maximum at FAl/uc $\simeq$ 34. It is not shown in Fig. 4A because this single point would have compressed the Y scale by a factor of 3. The rate obtained at FAl/uc = 51 is about the same as that obtained for FAl/uc = 2.6. Figure 4B, where the variable is Q_1/uc, reveals similar facts but Fig. 4C, where the variable is FAl1, shows a monotonous variation of activity. Indeed, the values of FAl1/uc for FAl/uc = 2.6 or 51 are approximately the same as those one can read on the line in Fig. 4A.

In addition, as shown in Fig. 3C, our experimental data obtained for *n*-pentane transformation are close to those obtained by Sohn *et al.* (6) for *n*-hexane. It may, thus, be suggested that these transformation in dealuminated Y are carried out by the strong Brønsted sites, but it is evident that more work is necessary before generalizing the conclusion.

TABLE 4

Summary of Activity Data for DHY

Sample	ACT-285 Total	ACT-285 Iso	ACT-285 Crack	Sel-Iso-285 (%)	ACT-350 Total	ACT-350 Iso	ACT-350 Crack	Sel-Iso-350 (%)	E^*tot (kJ/Mol)
DHY500	0.17	0.14	0.04	78	1.64	0.88	0.76	54	100 ± 2
DHY600	0.50	0.26	0.24	76	1.24	0.74	0.50	60	89 ± 7
DHY700	0.17	0.12	0.05	74	0.69	0.45	0.24	65	61 ± 7
DHY800	0.15	0.11	0.04	71	0.42	0.28	0.14	67	59 ± 4

Note. Act-285, Sel-Iso-285, Act 350, Sel-Iso-350, are the activity and selectivity to isomerization at 285 and 350°C, respectively. Iso, crack, and total are the rates of isomerization, cracking, and total transformation (unit: 10^{18} molecule/min/g). E^*tot is the activation energy of total transformation.

Note that in Figs. 4B, 2A, and 2B none of the reasonably linear regression goes to zero as it should. It looks like a fraction of sites (either Q_1 or FAl1) are not playing a role in the reaction, or that other kinds of sites (such as Lewis sites) must be taken into account. Because the Lewis acid site concentration is likely to increase as FAl decreases, compensation effects cannot be excluded.

The effect of steaming on the steady-state rate of pentane transformation was also examined. The activity of the steamed SDHZ samples is still within the range of the linear regression obtained for DHZ. Steaming does not considerably change the Si/FAl ratio.

For 10 samples, the *n*-pentane transformation has been studied at four temperatures in order to obtain the apparent activation energy. The Arrhenius plots were good and they show that the activation energy increases rapidly up to 110 kJ mol^{-1} as the ratio of the strongest sites (FAl1) to the total number of Brønsted sites (Q_1) decreases below 0.3, as shown in Fig. 5. The CO IR low-temperature study (20) has shown that in DHY there was a broad distribution of sites with different CO chemisorption energy. Thus, the heterogeneity of the active sites is larger than in the other zeolites. The increase in the activation energy with decreasing FAl1/Q_1, and the decrease of the rate when the number of sites decreases, affects the catalytic activity in opposite directions. This may be the reason why a maximum has also been observed for HY in plotting the activity vs FAl (1, 6, 18).

The activation energy observed for the overall transformation on the DHZ samples is consistently about 60

TABLE 5

Activity for Steamed Samples and the Sample after Partial Removal of NFAl

Sample	ACT-285 Total	ACT-285 Iso	ACT-285 Crack	Sel-Iso (%)
SDHZ0	21	2.0	17	9.5
SDHZ30	25	2.8	22	11.2
SDHZ150	23	2.4	20	10.4
SDHZ530	19	2.0	16	10.5
SDHZ1500	16	1.6	13	10.0
USYR	2.5	1.7	0.9	68.0
DHY600R	0.48	0.26	0.22	54.2
DHZ700R	11.6	1.9	9.8	16.4

Note. See Legends to Tables 3 and 4 for more information.

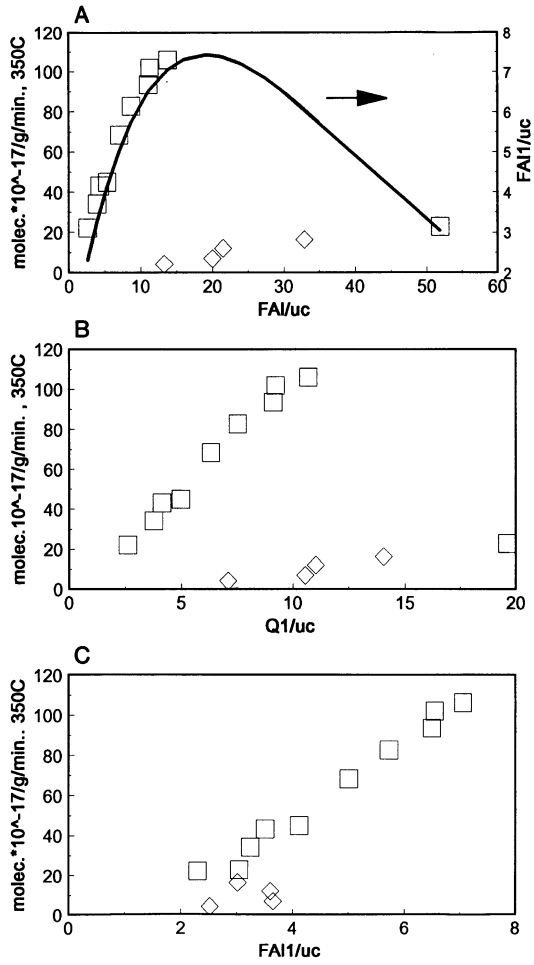

FIG. 4. Activity obtained by Sohn *et al.* (6), (□) for the transformation of hexane on dealuminated Y zeolite (at 350°C), transformation of pentane on DHY, (◇) our data. The line in (A) represents the variation of FAl1/uc vs FAl/uc. The same rates are in (A), (B), and (C); only the independent variable is changed.

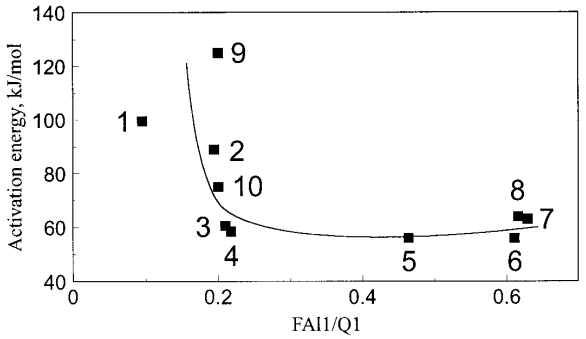

FIG. 5. Activation energy vs fraction of FAl1/Q_1. Points 1, 2, 3, 4, 5, 6, 7, 8, 9, and 10 correspond to the samples DHY500, DHY600, DHY700, DHY800, DHM500, DHZ400, DHZ500, DHZ600, and USY (double), respectively.

kJ/mol. The fraction of the strongest Brønsted sites (FAl1) is more than 50% of the total number of Brønsted sites (Q_1), since the Si/FAl ratios are larger than 15. The activation energy for pentane transformation and the product distribution at 10% conversion are listed in Table 6. The peculiar behavior of DHZ with respect to DHM and USY is evident. Similarly, Miale *et al.* (29) observed activation energies in the order to 120 kJ/mol on activated faujasites and mordenites (or "low silica" zeolites) in the cracking of hexane, while Zholobenko *et al.* (16) have obtained about 50–67 kJ/mol in the transformation of hexane on steamed ZSM-5. If the activation energy for isomerization or cracking were calculated separately we observed that the activation energy for the cracking of pentane is about 15 kJ/mol larger than the activation energy for isomerization. We have chosen to use the activation energy for the overall process because for DHZ, especially, the extent of the isomerization reaction was too low to yield accurate data.

In summary, the observations reported for DHY suggest that during dealumination the acid strength and catalytic activity increase as Si/FAl becomes larger than 5. Beyond that limit, the strength of Brønsted sites becomes approximately constant and the number of acidic OH groups related to FAl1 is the determining factor in catalytic activity.

The total activity with respect to FAl1 and Q_1 is larger for DHM than for DHZ (30). This would be unexpected if only Brønsted acid sites were involved. Indeed, DHZ should be more efficient because of the higher fraction of strongest Brønsted sites (FAl1/Q_1). The reason for the enhanced efficiency in DHM is probably due to the effect of the Lewis sites, as shown earlier (24).

The selectivity for isomerization is much lower for DHZ than for DHM, while on DHY and USY about 80% of the selectivity is toward isomerization. Cracking is more "acid" demanding and is favored by a high FAl1/Q_1 ratio. For each of the zeolites studied here the selectivity is approximately constant whatever the numbers of acid sites. This suggests that the selectivity is essentially structure dependent (30, 31).

The effect of the partial removal of NFAl in samples DHZ700R, DHY600R, and USYR decreases the activity of pentane transformation by about a nonsignificant 5%.

In Table 7, C5/*i*-C5, the ratios of the activity of pentane transformation over that of isopentane transformation are reported for USY, one dealuminated H-mordenite and the set of DHZ. This ratio is somewhat similar to the C6/3-MeC5 ratio used by Frilette *et al.* (32) as a constraint index (CI). The isopentane trnasformation was 12 times faster than the pentane transformation on USY. The ratio for DHM500 is 0.4 and larger than 0.6 for the ZSM-5 samples. This is consistent with the Mobil CI observed for different zeolites reported by Jacobs and Martens (33). With the increased calcination temperature of these samples, the fraction of mesopore volume over the total pore volume increases; thus, one may expect that the constraint effect should be smaller, as indeed observed, since the C5/*i*-C5 ratio decreased from 3 (DHZ400) to 0.6 (DHZ800).

TABLE 6

Product Distribution at 10% Conversion in H_2 Obtained with DHZ Samples and Comparison with H-mordenite and USY

Sample	C1 + C2 (%)	C3 (%)	*i*-C4 (%)	C4 (%)	*i*-C5 (%)	C6 (%)	E^*tot (kJ mol^{-1})
DHZ400	0	34	21	26	16	3	56 ± 8
DHZ500	0	34	17	30	16	3	64 ± 7
DHZ600	1	31	24	27	13	2	63 ± 3
DHZ700	0	33	24	28	13	2	—
DHZ800	3	32	21	24	14	6	—
DHZ900	45	12	11	14	13	5	—
DHM500	4	14	26	13	33	10	60 ± 3
USY	4	5	10	4	67	10	125 ± 13

Note. All numbers are in mol%. The temperature is 285°C.

TABLE 7

Isopentane Transformation

Sample	Act-I	Iso	C5/*i*-C5 (%)
DHZ400	8.5	0	3.1
DHZ500	8.2	1.3	1.7
DHZ600	11	3.9	1.3
DHZ700	8.2	5.5	1.7
DHZ800	2.7	8.0	0.6
DHZ900	0.31	17	1.0
DHM500	3.6	1.8	0.4
USY	31	57	0.08

Note. Act-I and Iso are the total activity and isomerization activity (10^{18} molecule/min/g). The selectivity of the isomerization reaction, C5/*i*-C5, is the ratio for the activity of pentane transformation to that of isopentane transformation at 285°C.

In an earlier study of the microporous characteristics of HY, HZSM-5, and H-mordenite dealuminated by calcination, it has been shown (25) that in DHY and DHZ, only a fraction of micropore volume is clogged by NFAl. Yet, in DHM, NFAl invades all the available voids, including those which are not available to N_2 or CO.

In DHY, due to the more open structure the clogging effect does not significantly influence the reaction rate, but in DHZ, the variation of the C5/*i*–C5 is rapid because the narrower size of the pores allows increased clogging by NFAl.

Several interesting points deserve to be outlined from the product distribution shown in Table 6. Only saturated hydrocarbons have been observed, indicating large hydrogen transfers.

(i) The fraction of isopentane is low at 285°C on DHZ in H_2 in agreement with the results in Table 3, showing that cracking is the dominant reaction.

(ii) The fraction of C6 is low, suggesting that the contribution of the disproportionation of the *i*-C5 dimer to isobutane and C6 is not significant.

(iii) The fraction (C1 + C2) is small except for DHZ900, where the C1 + C2 was the major cracking products. High C1 + C2 fractions could suggest a pentacoordinated carbonium cracking mechanism such as that proposed by Haag and Dessau (34), but that has been observed only once in this work, preventing any valid discussion.

The low contributions from both C1 + C2 and C6 can not be easily explained. Virtual absence of C1 and C2 products in low-temperature operating conditions, such as ours, for *n*-hexane cracking was also observed by Miale *et al.* (29). The dimer intermediate mechanism was proposed and high C6 concentration should be expected. This mechanism is compatible with the width of the pores of faujasite and mordenite, but it is less probable in ZSM-5.

In summary, the differences between ZSM-5 samples and USY and H-mordenite are (i) the selectivity to isomerization is much higher in USY and H-mordenite, and the C6 percentage in the products is much higher than that in ZSM-5 and (ii) the ratio of *i*-C4/C4 is closer to the equilibrium ratio in USY and H-mordenite.

CONCLUSIONS

One of the main conclusions of the study of the activity of dealuminated Y and ZSM-5 toward the transformation of pentane is the overpowering influence of the strong Brønsted sites (FAl1) located on a Si–OH–Al bridge in a cluster where the third coordination shell of the silicon does not contain aluminum.

If the ratio of FAl1 to the total number of Brønsted sites is large, the activation energy of the overall tranformation is about 60 kJ mol^{-1}, and the steady-state rate is proportional to FAl1 or Q_1. If the ratio FAl1/Q_1 is small, the activation energy is appreciably higher.

The clogging of the pore system by NFAl strongly influences the isopentane (*i*-C5) or pentane transformation in DHZ, as could have been anticipated from earlier data.

The selectivity toward isomerization is essentially structure dependent, for each set of zeolites it is almost constant, whatever the acid site concentration and activity.

ACKNOWLEDGMENTS

The financial support of the U.S. Department of Energy (Grant DE-FG02-90ER1430) is gratefully acknowledged. We also thank Dr. Alexander Blumenfeld and Dominique Coster for the ^{29}Si MAS NMR spectra. The authors are grateful to the reviewers who have pointed out some flaws in the original manuscript.

REFERENCES

1. Shertukde, P. V., Hall, W. K., Dereppe, J.-M., and Marcelin, G., *J. Catal.* **139**, 468 (1993).
2. Boudart, M., and Djega-Mariadassou, G., "Reaction Kinetics in Heterogeneous Catalysis," p. 199. Fudan Univ. Press, Shanghai, 1988.
3. Gates, B. C., "Catalytic Chemistry." Wiley, New York, 1992.
4. Aronson, M. T., Gorte, R. J., and Farneth, W. E., *J. Catal.* **98**, 434 (1986).
5. Olson, D. H., Haag, W. O., and Lago, R. M., *J. Catal.* **61**, 390 (1980).
6. Sohn, J. R., DeCanio, S. J., Fritz, P. O., and Lunsford, J. H., *J. Phys. Chem.* **90**, 4847 (1986).
7. Macedo, A., Auroux, A., Raatz, F., Jacquinot, E., and Boulet, R., *in* "Perspectives in Molecular Sieve Science" (W. H. Flank and T. E. Whyte, Jr., Eds.), p. 98. Am. Chem. Soc., Washington, DC, 1988.
8. Spiekwak, B. E., Handy, B. E., Sharma, S. B., and Dumesic, J. A., *Catal. Lett.* **23**, 207 (1994).
9. Auroux, A., Muscas, M., Coster, D. J., and Fripiat, J. J., *Catal. Lett.* **28**, 179 (1994).
10. Beaumont, R., and Barthomeuf, D., *J. Catal.* **26**, 239 (1972).
11. Kerr, G. T., and Miale, J. N., U.S. Patent 3,493,519, 1970.
12. Levitz, A., Blumenfeld, A., and Fripiat, J. J., *Catal. Lett.* **38**, 11 (1996).
13. Blumenfeld, A., Coster, D., and Fripiat, J. J., *J. Phys. Chem.* **99**, 15181 (1995).
14. Ashton, A. G., Batmanian, S., Clark, D. M., Dwyer, J., Fitch, F. R., Hinchcliffe, A., and Machado, F. J., *in* "Catalysis by Acid and Bases" (B. Imelik *et al.*, Eds.), p. 101. Elsevier, Amsterdam, 1985.
15. Lago, R. M., Haag, W. O., Mikovsky, R. J., Olson, D. H., Hellring, S. D., Schmitt, K. D., and Kerr, G. T., *in* "Proceedings of the 7th International Zeolite Conference" (Y. Murakami *et al.*, Eds.), p. 677. Kodansha, Tokyo, 1986.
16. Zholobenko, V. L., Kustov, L. M., Kazansky, B. V., Loeffler, E., Lohse, U., and Oehlmann, G., *Zeolites* **11**, 132 (1991); Zholobenko, V. L., Kustov, L. M., Kazansky, B. V., Loeffler, E., Lohse, U., Oehlmann, G., and Peuker, C. H., *Zeolites* **9**, 304 (1990).
17. Beyerlein, R. A., McVicker, G. B., Yacullo, L. N., and Ziemiak, J. J., *J. Phys. Chem.* **92**, 1967 (1988).
18. Carvajal, R., Chu, P.-J., and Lunsford, J. H., *J. Catal.* **125**, 123 (1990).
19. Coster, D., Ph.D. thesis, University of Wisconsin–Milwaukee, 1995.
20. Hong, Y., Ph.D. thesis, University of Wisconsin–Milwaukee, 1995.
21. Anderson, M. W., and Klinowski, J., *Zeolite* **6**, 455 (1986).
22. Gruver, V., and Fripiat, J. J., *J. Phys. Chem.* **98**, 8549 (1994) and references therein.
23. Gruver, V., Panov, A., and Fripiat, J. J., *Langmuir*, accepted.

24. Hong, Y., Gruver, V., and Fripiat, J. J., *J. Catal.* **150**, 421 (1994) and references therein.
25. Hong, Y., and Fripiat, J. J., *Microporous Mater.* **4**, 323 (1995).
26. Wang, Q. L., Giannetto, G., and Guisnet, M., *J. Catal.* **130**, 47 (1991).
27. ASTM 4842-88, "Annual Book of ASTM Standards." Vol. 05.03, p. 687. ASTM, Philadelphia, 1993.
28. Biaglow, A. I., Parrillo, D. J., Kokotailo, G. T., and Gorte, R. T., *J. Catal.* **148**, 213 (1994).
29. Miale, J. N., Chen, N. Y., and Weisz, P. B., *J. Catal.* **6**, 278 (1966).
30. Gruver, V., Hong, Y., Panov, A., and Fripiat, J. J., 11th International Congress on Catalysis, Baltimore, 1996, in press.
31. Hong, Y., Gruver, V., and Fripiat, J. J., *Div. Petrol. Chem. ACS* **40**, 590 (1995).
32. Frilette, V. J., Haag, W. O., and Lago, R. M., *J. Catal.* **67**, 218 (1981).
33. Jacobs, P. A., and Martens, J. A., *Stud. Surf. Sci. Catal.* **67**, 218 (1981).
34. Haag, W. O., and Dessau, R. M., "Proceedings, 8th International Congress on Catalysis, Berlin, 1984," p. 305. Dechema, Frankfurt-am-Main, 1984.